Chinese Chemical Letters 32 (2021) 2499–2502

Contents lists available at ScienceDirect

Chinese Chemical Letters

journal homepage: www.elsevier.com/locate/cclet

Communication

Stainless steel cloth modified by carbon nanoparticles of Chinese ink as scalable and high-performance anode in microbial fuel cell

Haoliang Wu[a], Hao Tan[a], Luye Chen[a], Bin Yang[a,b], Yang Hou[a,b], Lecheng Lei[a,b], Zhongjian Li[a,b,*]

[a] College of Chemical and Biological Engineering, Key Laboratory of Biomass Chemical Engineering of Ministry of Education, Zhejiang University, Hangzhou 310027, China
[b] Institute of Zhejiang University-Quzhou, Quzhou 32400, China

ARTICLE INFO

Article history:
Received 8 October 2020
Received in revised form 22 November 2020
Accepted 27 December 2020
Available online 31 December 2020

Keywords:
Chinese ink
Microbial fuel cell
Stainless steel
Polypyrrole
Carbon nanoparticles

ABSTRACT

Microbial fuel cells (MFCs) have various potential applications. However, anode is a main bottleneck that limits electricity production performance of MFCs. Herein, we developed a novel anode based on a stainless steel cloth (SC) modified with carbon nanoparticles of Chinese ink (CI) using polypyrrole (PPy) as a building block (PPy/CI/SC). After modification, PPy/CI/SC showed a 30% shorten in start-up time (36.4 ± 3.3 h *vs.* 52.3 ± 1.8 h), 33% increase in the maximum current (12.4 ± 1.4 mA *vs.* 9.3 ± 0.95 mA), and 2.3 times higher in the maximum power density of MFC (61.9 mW/m^2 *vs.* 27.3 mW/m^2), compared to Ppy/SC. Experimental results revealed that carbon nanoparticles were able to cover SC uniformly, owing to excellent dispersibility of carbon nanoparticles in CI. The attachment of carbon nanoparticles formed a fluffy layer on SC increased the electrochemically-active surface area by 1.9 times to 44.5 cm^2. This enhanced electron transfer between the electrode and bacteria. Further, embedding carbon nanoparticles into the PPy layer significantly improved biocompatibility as well as changed functional group contents, which were beneficial to bacteria adhesion on electrodes. Taking advantage of high mechanical strength and good conductivity, a large-size PPy/CI/SC was successfully prepared (50×60 cm^2) demonstrating a promising potential in practical applications. This simple fabrication strategy offers a new idea of developing low cost and scalable electrode materials for high-performance energy harvesting in MFCs.

Microbial fuel cells (MFCs) can convert chemical energy in wastewater into electricity with electrochemically active bacteria (EAB), which oxidize organic matter and donate electrons to electrodes [1]. MFCs have been considered to have great potentials in energy generation, wastewater treatment, and biosensors [2–4]. However, low electricity production is a main limiting factor for MFCs currently [5,6]. The electricity production performance is greatly affected by electron transfer between EAB and anodes. Therefore, electrochemical properties of electrode materials (*e.g.*, conductivity, biocompatibility and stability) have great impacts on the electricity production of MFCs [7–9]. In this regard, a lot of efforts have been made to develop novel anodes to improve the electricity production performance of MFCs [10,11].

Carbon nanomaterials, such as carbon nanotubes (CNTs), graphene and biomass-derived carbon nanoparticles, have been widely used to modify anodes. Many novel anodes have been developed by implementing carbon nanomaterials as modifiers and electricity production of MFCs was improved due to unique physical and chemical properties of different carbon nanomaterials [12–14]. First, carbon nanomaterials possess excellent conductivity which can enhance electron transfer between electrodes and microbes by lowering charge transfer resistance. Second, carbon nanomaterials provide high specific areas [15–17]. Although carbon nanomaterials are promising materials for modifying anodes, inert surfaces of most carbon nanomaterials causing poor dispersibility in aqueous solutions [18]. Besides, many carbon nanomaterials are prone to aggregate forming large-size clusters. For instance, individual CNTs inevitably form parallel bundles because of strong van der Waals interaction [19]. These properties result in ununiform modification layers. Also, high cost and complex fabrication processes hinder large-scale practical applications of carbon nanomaterials in electrodes modifications for

* Corresponding author at: College of Chemical and Biological Engineering, Key Laboratory of Biomass Chemical Engineering of Ministry of Education, Zhejiang University, Hangzhou 310027, China.
E-mail address: zdlizj@zju.edu.cn (Z. Li).

https://doi.org/10.1016/j.cclet.2020.12.048
1001-8417/

MFCs [20]. Hence, there is an urgent need to find a low-cost, readily available carbon nanomaterial with good dispersibility as a substitution.

Chinese ink (CI) has been used as writing material for a long history in China. It contains carbon nanoparticles ranging from 50 nm to 100 nm [21,22]. The carbon nanoparticles of CI come from soot obtained by burning wood and oil, which guarantee good biocompatibility. Also, CI contains animal glue which can provide a stable dispensability of carbon nanoparticles in liquid and preventing carbon nanoparticles from aggregating to form large-size clusters [18]. For these good properties, CI has been used to modify electrodes in MFCs recently. Zhou *et al.* developed an electrode through coating natural loofah sponge with CI and achieved a high current density [23]. However, the CI coated loofah sponge electrodes were prepared by simply dipping loofah sponge into CI and drying. The interaction between carbon nanoparticles and the substrate was not reliable enough during long-term operation. Although loofah sponge shows good biocompatibility, poor conductivity, weak mechanical strength, and difficulties in processing make it unlikely to be used in large scale applications. Therefore, using metal materials, such as stainless steel materials, as substrate and modified with CI is an ideal strategy [24]. However, it is difficult to build a solid connection between CI and stainless steel. Polypyrrole (PPy) is a kind of polymer with good conductivity, which can be synthesized easily through electropolymerization. PPy can incorporate various carbon nanomaterials and form PPy/carbon hybrid nanocomposites on electrode substrates in MFCs to improve electricity production performance [25,26]. The obtained nanocomposites maintain properties of both carbon nanomaterials and PPy, *e.g.*, high specific surface area and good conductivity. Therefore, PPy is a suitable building block to modify stainless steel substrates.

In this study, a novel and scalable MFC anode was developed by modifying stainless steel cloth (SC) with carbon nanoparticles of CI. PPy was used as a building block through electropolymerization. The characteristics of electrodes were obtained by scanning electron microscopy (SEM), X-ray photoelectron spectroscopy (XPS) and other methods. The obtained electrodes were tested in both MFCs and microbial three-electrode cells (M3Cs) to study the bioelectrochemical performance, including start-up time, maximum current, and polarization curves. Further, a large-size electrode was obtained with this method, demonstrating a promising potential in practical applications. This simple fabrication strategy offers a new idea of developing low cost and high-performance electrode materials for MFCs.

Carbon nanoparticles of CI can be homodispersed in the electrolyte for electropolymerization without any treatments, such as ultrasonic vibration. (Fig. S1a in Supporting information). This property came from that the glue in CI, working as a dispersing agent, made carbon nanoparticles suspend stably in liquid, which helped carbon nanoparticles attach to SC more uniformly. SEM images showed that CI consisted of small nanoparticles with a diameter ranging from 50 nm to100 nm (Fig. S1b in Supporting information).

After modification, the appearance of PPy/SC and PPy/CI/SC was different from that of SC (Fig. 1a). PPy/SC and PPy/CI/SC had a black layer covering the whole substrate uniformly. Compared with PPy/SC, PPy/CI/SC had a much darker color and fluffy structure. These differences came from the embedded carbon nanoparticles in the PPy layer. Since SC worked as a substrate, PPy/CI/SC possessed high mechanical strength and could be bent arbitrarily without detachment of modification layer. A large-size PPy/CI/SC (50×60 cm^2) was prepared successfully. Compare with bare SC, the large-size PPy/CI/SC was uniformly covered with a black rough layer (Fig. 1b). The modification layer on large-size PPy/CI/SC was the same in appearance as that on small-size ones. It proved this

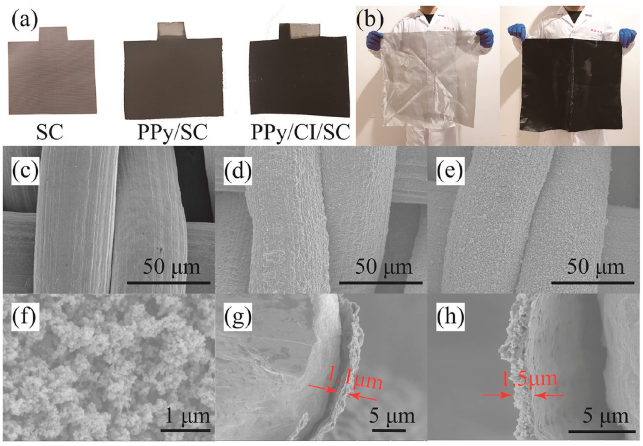

Fig. 1. (a) Photographs of SC, PPy/SC and PPy/1%CI/SC. (b) Large-size electrode before and after modification. SEM images of (c) SC, (d, g) PPy/SC and (e, f, h) PPy/1%CI/SC.

method, which could simply prepare large-size electrode with a uniform modification surface, had great potential in practical applications. SEM images showed that the SC possessed a smooth surface with strip texture along with the fiber (Fig. 1c). A rough PPy layer can be observed on PPy/SC (Fig. 1d). While, PPy/CI/SC possesses a rougher surface of PPy layer with embedded carbon nanoparticles, which could be beneficial to bacterial adhesion (Fig. 1e). The Elemental mapping images showed a uniform distribution of C, N, and O on PPy/CI/SC surface indicating that the PPy layer formed evenly on SC (Fig. S2 in Supporting information). SEM images with higher magnification further confirmed that there were large amounts of carbon nanoparticles, with diameters ranging from 50 nm to 100 nm, embedded on the surface of PPy/CI/SC (Fig. 1f). Cross-sectional images showed the thickness of the layer was around 1.1 μm on PPy/SC and around 1.5 μm on PPy/1%CI/SC (Figs. 1g and h). These phenomena proved that carbon nanoparticles of CI were incorporated by PPy forming nanocomposites during electropolymerization. By coupling CI and PPy electropolymerization, carbon nanoparticles can be uniformly modified onto SC.

XPS revealed that compared with PPy/SC, the content of C elements on the surface of PPY/CI/SC increased, while N-content decreased and O-content almost remained at the same level (Table S1 in Supporting information). O 1s spectrum of both PPy/SC and PPy/CI/SC presented two kinds of oxygen functionalities, C—O centering at 532.6 eV and C=O centering at 531.3 eV (Fig. 2a) [27–30]. The ratio of C—O and C=O content was almost the same. The high content of C=O, which is a hydrophilic group, may provide biocompatible condition for bacteria to attach and move on the electrode surface [31]. As for N, N 1s spectrum presented two kinds of N-functionalities, protonation pyrrolic N centered at 400.4 eV and neutral pyrrole N centered at 399.2 eV (Fig. 2b) [28–30,32]. The category of N-functionalities did not change after modification. As the total N content decreased, pyrrolic N content on PPy/CI/SC was lower than PPy/SC. It is reported pyrrolic nitrogen (N-5) has negative impacts on bacterial adhesion and electron transfer for their negatively charged property [33]. Therefore, PPy/CI/SC may show better biocompatibility than PPy/SC theoretically. C 1s spectrum was presented three kinds of peaks (287.6, 285.3, and 283.9 eV), which were C=O, C-N and C-C respectively (Fig. S3 in Supporting information).

Zeta potential is another important factor that influents bacterial adhesion on the anode. All fabricated electrodes were positively charged, which were beneficial to attaching negative-charged EAB (Fig. 2c). Conductivity of anodes influents the

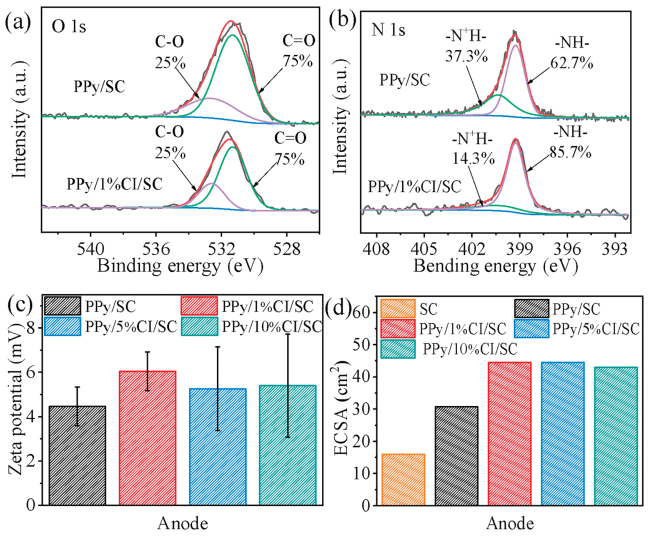

Fig. 2. High-resolution spectrum of O 1s (a) and N 1s (b) peak of the PPy/SC and PPy/1%CI/SC respectively. Zeta potential (c) and electrochemical active surface area (d) of studied electrodes.

electricity generation performance of MFCs. The conductivity test result showed the modified electrodes maintained the good conductivity of SC (Fig. S4 in Supporting information). After modification, the charge transfer resistance (R_{ct}) of PPy/SC, PPy/1%CI/SC, PPy/5%CI/SC, PPy/10%CI/SC were 0.46, 0.44, 0.43, 0.23 Ω respectively, which were lower than that of SC (4.74 Ω, Fig. S5 in Supporting information). After modification, conductivity increased and R_{ct} reduced accordingly. Electrochemically-active surface area (ECSA) also affects the electricity production performance of MFCs. PPy/CI/SC had a large ECSA around 44.5 cm^2, which was significantly higher than PPy/SC (30.7 cm^2) and SC (16 cm^2) (Fig. 2d). With the help of the rough and three-dimensional PPy/CI modification layer, more active sites for electron transfer were provided.

To investigate the bioelectrochemical performance of different electrodes, chronoamperometry (CA) was conducted in triplicate in M3Cs. A typical cycle of each electrode was presented in Fig. 3a, which showed PPy/1%CI/SC had a shorter start-up time and higher maximum current compared with PPy/SC. M3C with PPy/CI/SC reached exponential stage earlier than PPy/SC. The start-up time of PPy/1%CI/SC (36.4 ± 3.3 h) was reduced by 33% compared with PPy/SC (52.3 ± 1.8 h). The average maximum current of PPy/1%CI/SC (12.4 ± 1.4 mA) was 1.33 times of PPy/SC (9.3 ± 0.95 mA, Fig. 3b). The porous and open structure of nanocomposites formed by PPy and carbon nanoparticles could provide larger a ECSA for PPy/1%CI/SC [34]. The porous surface together with higher ECSA was beneficial to more efficient interactions between electrode and bacteria, high bacterial loading, and eventually building a solid conductive matrix with bacteria on the electrode. This formed biofilm would facilitate extracellular electron transfer from bacterium membrane c-type cytochromes or mediators to electrode surfaces [35,36]. In the CA test, the relationship between the concentration of CI and electrodes properties was explored. The result showed that a higher concentration than 1% of CI did not increase the maximum current or shorten start-up time in M3Cs obviously (Fig. 3b and Fig. S6 in Supporting information). It is likely because 1% CI is enough to modify the SC with a geometric area of 2.5 cm × 3 cm. Therefore, only PPy/1%CI/SC was tested for electrochemical performance in the MFC test.

The electricity production performance of PPy/SC and PPy/1%CI/SC in MFCs is illustrated in Fig. 3c. Typical electricity generation curves were obtained. PPy/1%CI/SC (31 h) showed a much shorter start-up time than PPy/SC (81 h). As well, the MFC with a PPy/1%CI/SC anode showed more stable and reproducible electricity production cycles than that with a PPy/SC anode in a 400 h period operation. In four continuous cycles, the electricity production did not decay obviously with the PPy/1%CI/SC anode and each cycle lasted for about 70 h. While, for the PPy/SC anode, the electricity production reached the maximum at about 150 h. After that, the produced electricity decreased to almost 0 mA at about 400 h. Also, each cycle showed a much shorter and uneven period of time than the PPy/1%CI/SC anode. The maximum output voltage produced under 1000 Ω with a PPy/1%CI/SC anode was 0.337 V and that of a PPy/SC anode was 0.297 V. To evaluate the electricity production performance of the MFCs with different anodes, when output voltage was in the steady stage, polarization and power density curves were measured. The MFC with a PPy/1%CI/SC anode showed a higher maximum power density of 61.9 mW/m^2 compared with that with a PPy/SC anode of 27.3 mW/m^2 (Fig. 3d). PPy/1%CI/SC anode was lower than the internal resistance of the MFC with a PPy/SC anode. All these results proved that PPy/1%CI/SC had better electricity production performance than PPy/SC, which consisted with the CA test. It is believed that the carbon nanoparticles of CI played a key role in the improvements. The CI could change surface characteristics of electrodes, such as content of different functional groups. Besides, the embedded carbon nanoparticles in PPy layer could greatly improve ECSA of electrodes and provide more porous and rough surfaces for initial bacterial adhesion, resulting in shorter start-up time. After the formation of the biofilm, the embed carbon nanoparticles helped to build connections between bacteria and form a conductive bacteria-carbon nanoparticles-PPy matrix for more efficient electron transfer between EAB and the electrodes. As a result, MFC with PPy/1%CI/SC exhibited better electricity production performance.

After operating for more than 150 h in M3C, pink biofilms were observed on PPy/SC and PPy/CI/SC. SEM was conducted to further investigate EAB biofilm formed on electrodes. The most bacteria on electrodes were bacilliform. Since sodium acetate was the only substance and anaerobic condition was maintained during the whole operation, *Geobacter sulfurreducens* very possibly

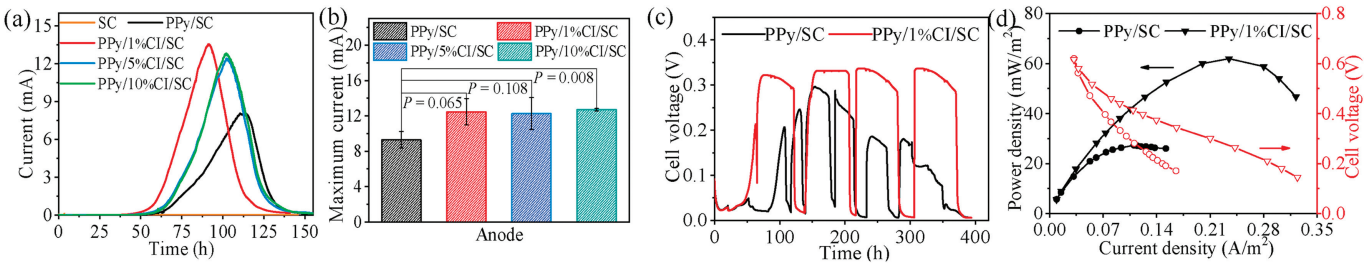

Fig. 3. (a) Chronoamperometric current *versus* time at a potential of 0.1 V. (b) Bar graph of the maximum current production in M3Cs with statistics. (c) Voltage output and polarization curves and (d) power density curves of MFCs equipped with various anodes.

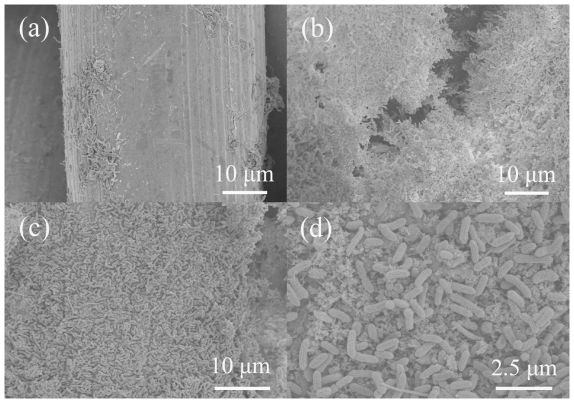

Fig. 4. SEM images of biofilms on (a) SC, (b) PPy/SC, (c, d) PPy/CI/SC.

dominated electrodes. For poor biocompatibility of SC, there was no obvious biofilm observed (Fig. 4a). After coating with the PPy layer, biocompatibility was greatly improved. As a result, biofilms were detected both on PPy/SC and PPy/CI/SC (Figs. 4b and c). Although thick biofilms were on both PPy/SC and PPy/CI/SC, the one on PPy/CI/SC was more uniform. It is likely because the uniformly embedded carbon nanoparticles in PPy layer are beneficial to form an even biofilm on electrodes. The SEM image of PPy/CI/SC with a higher magnification showed complex connections between bacteria and nanocomposites (Fig. 4d). It confirmed the solid conductive matrix was formed on PPy/CI/SC. The rough surface created by embedding carbon nanoparticles provided a large number of sites for bacteria to adhesion. Plenty of nanoscale channels were exhibited in the matrix, which could accelerate the substrate transfer inside the biofilm [34]. As well, the matrix intimately contacted to bacteria supplying more activity sites for direct extracellular electron transfer. Therefore, the unique structure of the hybrid biofilm with nanocomposites was advantageous to bacterial adhesion, substrate diffusion, and extracellular electron transfer. Also, many microbial nanowires (or pili), which have been recognized as an important conduit between bacteria and extracellular electron acceptors, were observed [37]. It provided a good condition for electron transfer on PPy/CI/SC.

In this study, CI was used to modify SC with PPy as a building block. Beneficial from the excellent dispersibility of carbon nanoparticles in CI, a carbon nanoparticles uniformly embedded PPy layer was modified onto SC. With this simple modification method, a large-size PPy/CI/SC electrode was prepared. The characterization of electrodes indicated that modification increased ECSA while maintained high mechanical strength and conductivity. The XPS results revealed a decrease in pyrrolic-N content, which was beneficial to bacterial adhesion and electron transfer. The M3C equipped with PPy/CI/SC showed a shorter start-up time and higher maximum output current compared with PPy/SC. It indicated that PPy/CI/SC possessed better biocompatibility and electricity generation performance. The MFC test further confirmed that PPy/CI/SC had better bioelectrochemical performance as the maximum power density was 2.3 times higher than PPy/SC. The SEM images of biofilms proved that PPy/CI/SC exhibited better biocompatibility and bacterial adhesion compared to SC and PPy/SC. Modification SC with CI provides a new idea to develop scalable, low-cost, and high-performance anodes for energy harvesting in MFCs.

Declaration of competing interest

The authors declare that they have no known competing financial interests or personal relationships that could have appeared to influence the work reported in this paper.

Acknowledgments

This project was supported by the Zhejiang Provincial Key Research and Development Program (No. 2019C03102), the China Major Science and Technology Program for Water Pollution Control and Treatment (No. 2017ZX07101003), the National Natural Science Foundation of China (Nos. 21961160742, 22075245), and the Ministry Department of Zhejiang Province (No. Y201534982).

Appendix A. Supplementary data

Supplementary material related to this article can be found, in the online version, at doi:https://doi.org/10.1016/j.cclet.2020.12.048.

References

[1] B.E. Logan, B. Hamelers, R. Rozendal, et al., Environ. Sci. Technol. 40 (2006) 5181–5192.
[2] D. Pant, G. Van Bogaert, L. Diels, K. Vanbroekhoven, Bioresour. Technol. 101 (2010) 1533–1543.
[3] L. He, P. Du, Y. Chen, et al., Renew. Sust. Energy Rev. 71 (2017) 388–403.
[4] M. Di Lorenzo, T.P. Curtis, I.M. Head, K. Scott, Water Res. 43 (2009) 3145–3154.
[5] S. Choi, Biosens. Bioelectron. 69 (2015) 8–25.
[6] H. Wang, J.D. Park, Z.J. Ren, Environ. Sci. Technol. 49 (2015) 3267–3277.
[7] Y. Hindatu, M.S.M. Annuar, A.M. Gumel, Renew. Sust. Energy Rev. 73 (2017) 236–248.
[8] X. Xie, L. Hu, M. Pasta, et al., Nano Lett. 11 (2011) 291–296.
[9] J.M. Sonawane, A. Yadav, P.C. Ghosh, S.B. Adeloju, Biosens. Bioelectron. 90 (2017) 558–576.
[10] L. Yang, G. Yi, Y. Hou, et al., Biosens. Bioelectron. 141 (2019) 111444.
[11] M. Lu, Y. Qian, C. Yang, et al., Nano Energy 32 (2017) 382–388.
[12] T. Zhang, Y. Zeng, S. Chen, X. Ai, H. Yang, Electrochem. Commun. 9 (2007) 349–353.
[13] Y. Qiao, C.M. Li, S.J. Bao, Q.L. Bao, J. Power Sources 170 (2007) 79–84.
[14] M. Li, S. Ci, Y. Ding, Z. Wen, Sustain. Energy Fuels 3 (2019) 3415–3421.
[15] Q. Zhang, J.Q. Huang, W.Z. Qian, Y.Y. Zhang, F. Wei, Small 9 (2013) 1237–1265.
[16] M.F.L. De Volder, S.H. Tawfick, R.H. Baughman, A.J. Hart, Science 339 (2013) 535–539.
[17] Y. Xia, J. Feng, S. Fan, W. Zhou, Q. Dai, Chemosphere 263 (2021) 128069.
[18] W.L. Yan, A. Dasari, L.B. Kong, Compos. Part A: Appl. Sci. Manuf. 61 (2014) 209–215.
[19] D. Bouchard, W. Zhang, T. Powell, U.S. Rattanaudompol, Environ. Sci. Technol. 46 (2012) 4458–4465.
[20] Q. Chen, W. Pu, H. Hou, et al., Bioresour. Technol. 249 (2018) 567–573.
[21] H.C. Yang, Z.W. Chen, Y.S. Xie, et al., Adv. Mater. Interfaces 6 (2019) 1801252.
[22] J.R. Swider, V.A. Hackley, J. Winter, J. Cult. Herit. 4 (2003) 175–186.
[23] L.H. Zhou, L.H. Sun, P. Fu, C.L. Yang, Y. Yuan, J. Mater. Chem. A 5 (2017) 14741–14747.
[24] S.F.N. Rusli, M.H. Abu Bakar, K.S. Loh, M.S. Mastar, Int. J. Hydrogen Energy 44 (2019) 30772–30787.
[25] N. Khan, A.H. Anwer, A. Ahmad, et al., ACS Omega 5 (2020) 471–480.
[26] G. Wu, H. Bao, Z. Xia, et al., J. Power Sources 384 (2018) 86–92.
[27] N. Zhao, Z. Ma, H. Song, Y. Xie, M. Zhang, Electrochim. Acta 296 (2019) 69–74.
[28] X. Jian, M. He, L. Chen, et al., Electrochim. Acta 318 (2019) 820–827.
[29] X. Jian, H.M. Yang, J.G. Li, et al., Electrochim. Acta 228 (2017) 483–493.
[30] S. Misra, M. Bharti, A. Singh, et al., Mater. Res. Express 4 (2017) 085007.
[31] F. Yu, C. Wang, J. Ma, Electrochim. Acta 259 (2018) 1059–1067.
[32] Q. Liu, J. Zhu, L. Tan, et al., Dalton Trans. 45 (2016) 9166–9173.
[33] S. Cheng, W. Liu, D. Sun, H. Huang, Surf. Interface Anal. 49 (2017) 410–418.
[34] P. Zhang, J. Liu, Y. Qu, et al., J. Power Sources 361 (2017) 318–325.
[35] C.-e. Zhao, J. Wu, Y. Ding, et al., ChemElectroChem 2 (2015) 654–658.
[36] M. Eguílaz, A. Gutiérrez, G. Rivas, Sens. Actuators B: Chem. 225 (2016) 74–80.
[37] D.R. Lovley, Energy Environ. Sci. 4 (2011) 4896–4906.